Laser and Particle Beams (2015), *33*, 577–589.

doi:10.1017/S0263034615000701

Introducing a two temperature plasma ignition in inertial confined targets under the effect of relativistic shock waves: The case of DT and pB^{11}

SHALOM ELIEZER,[1] ZOHAR HENIS,[2,3] NOAZ NISSIM,[2] SHIRLY VINIKMAN PINHASI,[4] AND JOSÉ MARIA MARTINEZ VAL[1]

[1]Nuclear Fusion Institute, Polytechnic University of Madrid, Madrid, Spain
[2]Applied Physics Division, Soreq NRC, Yavne, Israel
[3]Racah Institute of Physics, Hebrew University, Israel
[4]42 Beery, Rehovot, Israel

(Received 6 May 2015; Accepted 16 June 2015)

Abstract

A criterion for a two temperature plasma nuclear fusion ignition is derived by using a common model. In particular, deuterium-tritium (DT) and proton–boron11 (pB^{11}) are considered for pre-compressed plasma. The ignition criterion is described by a surface in the three-dimensional space defined by the electron and ion temperatures T_e, T_i, and the plasma density times the hot spot dimension, $\rho \cdot R$. The appropriate fusion ion temperatures T_i are larger than 10 keV for DT and 150 keV for pB^{11}. The required value of $\rho \cdot R$ for pB^{11} ignition is larger by a factor of 50 or more than for DT, depending on the electron temperature. Furthermore, our ignition criterion obtained here for pB^{11} fusion is practically impossible for equal electron and ion temperatures. In this paper it is suggested to use a two temperature laser induced shock wave in the intermediate domain between relativistic and non-relativistic shock waves. The laser parameters required for fast ignition are calculated. In particular, we find that for DT case one needs a 3 kJ/1 ps laser to ignite a pre-compressed target at about 600 g/cm^3. For pB^{11} ignition it is necessary to use more than three orders of magnitude of laser energy for the same laser pulse duration.

Keywords: Fast ignition; Fusion; Laser; Relativistic shock wave; Two temperatures

1. INTRODUCTION

One of the approaches to solve the energy problem is the well-known inertial confinement fusion (ICF) driven by high power lasers. The physics of ICF is based on compressing and igniting rather than confining the fuel (Nuckolls *et al*., 1972; Atzeni & Meyer-Ter-Vehn, 2004; Velarde & Carpintero-Santamaria, 2007). In order to ignite the fuel with less energy it was suggested to separate the drivers that compress and ignite the target (Basov *et al*., 1992; Tabak *et al*., 1994). First the fuel is compressed to high density, then a second short pulse driver heats and ignites a small part of the fuel, the "hot spot" or "igniter", while the α-particles created in the nuclear interaction heat and burn the rest of the target. This idea is called fast ignition. The fast ignition problem is that the short laser pulse does not penetrate directly into the compressed target; therefore many schemes have been suggested (Guskov, 2013) to solve this issue. Presently from all the known fast ignition schemes the simplest fast ignition seems to be an "extra shock" wave (Betti *et al*., 2007; Eliezer & Martinez Val, 2011).

We suggested recently a novel shock wave ignition scheme (Eliezer *et al*., 2014a) where the ignition shock wave is generated in a pre-compressed target by the ponder-motive force of a high irradiance laser pulse. The shock wave velocity in this scheme is in the intermediate domain between the relativistic and non-relativistic hydrodynamics. Here, this fast ignition scheme is further developed and analyzed for deuterium-tritium (DT) and proton–boron11 (pB^{11}) fuels.

The interaction of a high power laser with a planar target creates a one-dimensional (1D) shock wave (Fortov & Lomonosov, 2010; Eliezer, 2013). The theoretical basis for laser induced shock waves analyzed and measured experimentally so far is based on plasma ablation. For laser intensities 10^{12} W/cm^2 < I_L < 10^{16} W/cm^2 and nanoseconds pulse duration a hot

Address correspondence and reprint requests to: Shalom Eliezer, Nuclear Fusion Institute, Polytechnic University of Madrid, Madrid, Spain. E-mail: noaznissim@gmail.com

plasma is created. This plasma exerts a high pressure on the surrounding material, leading to the formation of an intense shock wave moving into the interior of the target (Eliezer, 2002). In this paper we are interested in laser irradiances $I_L > 10^{21}$ W/cm^2. Shock waves induced by lasers with irradiances in this regime are described by relativistic hydrodynamics (Landau & Lifshitz, 1987). Relativistic shock waves were first analyzed by Taub (1948). Relativistic shocks may be a new route for fast ignition (Eliezer, 2012) and these shocks may be of importance in intense stellar explosions or in collisions of extremely high energy nuclear particles.

The shock wave created in a 1D target by the ponderomotive force[1] induced by very high laser irradiance, considered in this paper, is summarized schematically in Figure 1. In this domain of laser intensities the pondermotive force accelerates the electrons forward, so that the charge separation field forms a double layer (DL), in which the ions are accelerated forward. Figure 1a displays the capacitor model for laser irradiances I_L, where the ponderomotive force dominates the interaction; Figure 1b shows the system of the negative and positive layers DL, n_e and n_i are the electron and ion densities, accordingly, E_x is the electric field, λ_{DL} is the distance between the positive and negative DL charges, and δ is the solid density skin depth of the foil. The DL is geometrically followed by neutral plasma where the electric field decays within a skin depth and a shock wave is created. The shock wave description in the laboratory frame of reference is given in Figure 1c. This DL acts as a piston driving a shock wave (Naumova *et al*., 2009; Eliezer *et al*., 2014b; 2014c), moving in the unperturbed plasma. This model is supported in the literature by particle in cell simulation (Esirkepov *et al*., 2004; Naumova *et al*., 2009) and independently by hydrodynamic two fluid simulations (Hora *et al*., 1984; Hora, 1991; Lalousis *et al*., 2012; 2013). Here, it is proposed to use the above shock wave as igniter for pre-compressed fuel in the framework of fast ignition. Fast ignition of DT and pB^{11} fuels using ultra-intense short pulse laser was suggested and elaborated by Hora and collaborators (Hora *et al*., 2014; Lalousis *et al*., 2014). Their approach is based on impact of plasma blocks, generated by laser pulses shorter than picosecond and powers in the range of petawatt approaching exawatt, with solid targets. Recently, it was suggested that the above approach based on plasma blocks combined with ultra-high magnetic fields may reduce the required laser pulse power to lower values (Hora *et al*., 2014; 2015). Fast ignition of DT with ultra-intense laser pulse induced by accelerated protons by the DL described above was considered by Naumova *et al*., 2009.

Relativistic or non-relativistic (Zeldovich & Raizer, 1966) shock wave is described by five variables: The density ρ, the pressure P, the energy density e, the shock wave velocity u_s

[1]Kelvin's ponderomotion for electrostatics had to be generalized for laser–plasma interaction by Maxwell's stress tensor including the dielectric properties of plasmas. An example on how all components of the tensor had to be used is in Cicchitelli *et al*. (1990) and Eliezer (2002).

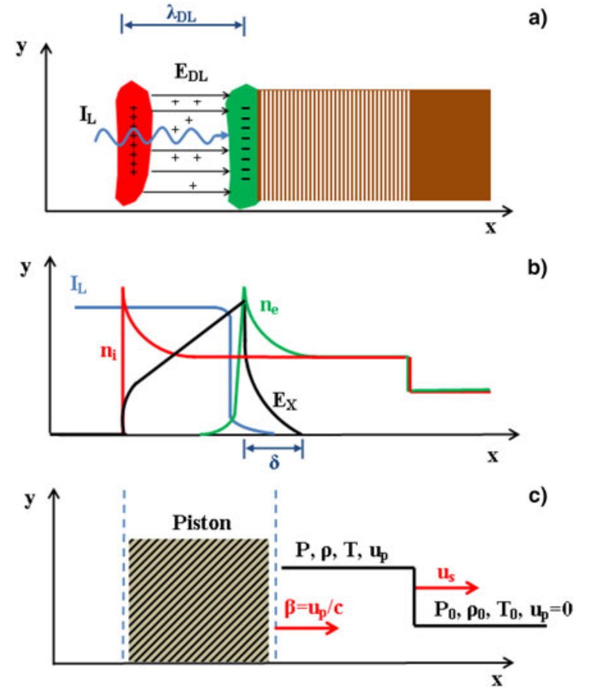

Fig. 1. (a) The capacitor model for laser irradiances I_L where the ponderomotive force dominates the interaction. (b) n_e and n_i are the electron and ion densities, accordingly, E_x is the electric field, λ_{DL} is the distance between the positive and negative DL charges, and δ is the solid density skin depth of the foil. The shock wave description in the laboratory frame of reference is given in (c).

and the particle flow velocity u_p, assuming that we know the initial condition of the target (ρ_0, P_0, e_0, and, the particle flow velocity u_0) before the shock arrival. The four equations relating the shock wave variables are the three Hugoniot relations describing the conservation laws of energy, momentum, and particles and the equation of state (EOS) connecting the thermodynamic variables of the state under consideration. The fifth equation necessary to solve the problem is obtained in a model where the pressure is induced by the laser ponderomotive force and its strength is a function of the laser pulse parameters. These equations for the relativistic and non-relativistic case are given in Appendix A (Eliezer *et al*., 2014b).

An ignition criterion for density-dimension product of the hot spot is calculated for non-equilibrium conditions where the electrons and ions temperatures are different, characteristic for fast ignition schemes. Electron and ion relaxation times relevant for these conditions are given in Appendix B. The equation describing the equality between nuclear fusion and energy losses is solved and the solution describes a surface in the 3D space of $\rho \cdot R$-T_e-T_i, where ρ and R are the igniter density and dimension, accordingly, T_e and T_i are the electron and ion temperatures. The emission of bremsstrahlung into the hydrodynamics was well included in the computations of block ignition by Chu (1972) and the subsequent numerous computations (Lalousis *et al*., 2013; 2014). In this paper, we solve the ignition criterion for the general case where the electron and ion temperatures are not necessarily equal and the solution is not dependent on a specific fast ignition scheme. The energy balance equation for DT plasma was considered in the literature for the DT case with equal electron and ion temperatures (Guskov *et al.*, 1976; Lindl, 1988; Takabe *et al.*, 1989; Rozanov *et al.*, 1995). This is in contrast to the genuine two-fluid hydrodynamics with explicit appearance of the internal electric fields in plasmas (Lalousis & Hora, 1983; Hora *et al.*, 1984; Eliezer *et al.*, 1995).

In the second part of this paper our model for fast ignition is described, based on two temperature laser induced shock wave in the intermediate domain between relativistic and non-relativistic shock waves. The laser parameters required for fast ignition of DT and pB^{11} fuels are calculated.

Section 2 describes the ignition criterion and Section 3 presents a two-temperature model for laser induced shock waves. Application of this model for DT and pB^{11} is presented in Section 4. The paper is concluded in Section 5.

2. THE IGNITION CRITERION

We analyze the nuclear fusion reactions

$$A_1 + A_2 \rightarrow A_3 + A_4 + E_f \qquad E_f = E_\alpha + E_{\text{others}} \tag{1}$$

E_f is the fusion energy in each reaction, E_α is α-particles energy usually deposited in part into the ignition domain and E_{others} is the energy contained in the other particles and practically not contained in the ignition volume under consideration. The ignition fusion power W_f [erg/(cm^3·s)] is given by

$$W_f\left[\frac{\text{erg}}{\text{cm}^3\cdot\text{s}}\right] = n_1 n_2 <\sigma v>_{12} E_\alpha \tag{2}$$

where n_1 and n_2 are the appropriate densities of particles A_1 and A_2, σ is the cross-section of reaction (1), $<\sigma v>_{12}$ is the fusion rate of this reaction and E_α is α-particles energy.

In general, not all of the α-fusion energy is deposited into the igniter. We define by f_α the fraction of the α-particles created and deposited into the igniter domain, while $(1-f_\alpha)$ is the escape fraction to the surrounding cold fuel. The value of f_α can be approximated by (Guskov & Rozanov, 1993)

$$f_\alpha = \begin{cases} \frac{3}{2}x_\alpha - \frac{4}{5}x_\alpha^2 & x_\alpha < \frac{1}{2} \\ 1 - \frac{1}{4x_\alpha} + \frac{1}{160 x_\alpha^3} & x_\alpha \geq \frac{1}{2} \end{cases} \qquad x_\alpha(\tau) = \frac{R}{R\alpha} \tag{3}$$

The igniter dimension R in our model is taken to be

$$R = \left(\frac{u_s}{c} - \frac{u_p}{c}\right) c\tau_L \tag{4}$$

where u_s and u_p are the shock wave velocity and the particle velocity accordingly, τ_L is the laser pulse duration that causes ignition and c is the speed of light. The velocities u_s and u_p depend on the laser and fuel parameters, as it is shown in Appendices A and C. The α range R_α is approximated for DT (Atzeni & Meyer-Ter-Vehn, 2004) and for pB^{11} by (Eliezer & Martinez Val, 1998) by:

$$DT\ \text{fusion:} \quad R_\alpha[\text{cm}] = \frac{1}{\kappa\rho_0}\left[\frac{1.5\times10^{-2} T_e(\text{keV})^{5/4}}{1 + 8.2\times10^{-3} T_e(\text{keV})^{5/4}}\right]$$
$$pB11\ \text{fusion:} \quad R_\alpha[\text{cm}] = \frac{a}{\rho}\left(\frac{T_e}{c}\right)^b \tag{5}$$
$$\begin{cases} T_e < 50\,\text{keV}: a = 0.25, b = 0.79, c = 10\,\text{keV} \\ T_e \geq 50\,\text{keV}: a = 1.1, b = 0.31, c = 100\,\text{keV} \end{cases}$$

The initial density of the pre-compressed target is ρ_0 and κ is the shock wave compression during the fast ignition process.

The equation describing the ignition requirement is given by

$$W_f - \sum W(\text{losses}) \geq 0 \tag{6}$$

The power density losses, W (losses), include the power densities of the mechanical work (W_m), bremsstrahlung radiation (W_B), and the heat wave transport by electrons (W_{he}). The ignition criteria are derived by explicitly writing Eq. (6) in the following way

$$f_\alpha W_f - W_B - W_{he} - W_m \geq 0 \tag{7}$$

The solution of the equality of Eq. (7) describes a surface in the 3D space of ρ-R-T_e-T_i. The ignition criterion (7) is solved for the general case where the electron and ion temperatures are not necessarily equal, extending previous studies for the DT case with equal electron and ion temperatures (Guskov *et al.*, 1976; Lindl, 1988; Takabe *et al.*, 1989; Rozanov *et al.*, 1995).

The bremsstrahlung power density losses W_B are given by

$$W_B\left[\frac{\text{erg}}{\text{cm}^3\cdot\text{s}}\right] = 1.5\times10^{-25} n_e \sum_{k=1,2} n_k Z_k^2 T_e(\text{eV})^{1/2}\left(1 + \frac{2T_e(\text{eV})}{500,000}\right) \tag{8}$$

Z_k is the charge number of particle k, n_e, and n_k are the electron density and the ion densities of particle k, accordingly. The second term in the right-hand side of Eq. (8) stems from the relativistic corrections to the bremsstrahlung losses. The heat conduction losses from the igniter domain are approximated by (Chu, 1972; Rozanov *et al.*, 1995):

$$W_{he}\left[\frac{\text{erg}}{\text{cm}^3\cdot\text{s}}\right] = \frac{K_e T_e}{R^2} = \frac{3.11\times10^9 T_e(\text{eV})^{7/2}}{R^2 \ln\Lambda} \tag{9}$$

The plasma logarithmic term lnΛ is

$$\ln\Lambda = 24 - \ln\left[\frac{n_e^{1/2}}{T_e(\text{eV})}\right] \tag{10}$$

In the solution of Eq. (7), a constant value $\ln\Lambda = 3.5$ was taken, appropriate for very high densities where the plasma is strongly coupled.

The mechanical expansion power losses are estimated by (Eliezer & Martinez Val, 1998)

$$W_m = \frac{2\rho v_m{}^3}{R}$$
$$W_m\left[\frac{\text{erg}}{\text{cm}^3\cdot\text{s}}\right] = \frac{2}{\rho^{1/2}R}\left(\frac{k_B T_e n_e + k_B T_i n_i}{\beta_m}\right)^{3/2} \tag{11}$$

The flow expansion velocity from the hot spot to the cold environment velocity, v_m, is consistent with an isochoric pre-compression of the target. As the pressure in the hot region P is higher than the pressure in the cold region, a shock wave will develop in the cold target according to the momentum conservation law

$$P \approx \beta_m \rho v_m{}^2 \tag{12}$$

Using the ideal gas EOS

$$P = k_B T_e n_e + k_B T_i n_i \tag{13}$$

and Eq. (12) we get the second of Eq. (11). For cases of an ionized pre-compressed target considered here the value $\beta_m = 4/3$ was used.

Substituting Eqs. (8), (9), (11) into Eq. (7) and multiplying by R^2 we get the following quadratic equation in $\rho\cdot R$

$$a(T_e, T_i)(\rho\cdot R)^2 + b(T_e, T_i)(\rho\cdot R) + c(T_e) \geq 0 \tag{14}$$

The solution of this inequality gives the ignition criterion as described in the domain above the surface in the 3D space of $\rho\, R$-T_e-T_i. In the following, Eq. (14) is written explicitly and solved for two cases: The DT and pB^{11} nuclear fusion fuel.

The DT case

$$D + T \rightarrow n + \alpha + 17,589\text{keV} \tag{15}$$

Equal density numbers for deuterium and tritium n_D and n_T, accordingly are assumed.

$$n_e[\text{cm}^{-3}] = n_i[\text{cm}^{-3}] = \left(\frac{\rho}{2.5 m_p}\right) = 2.39\times10^{23}\rho \tag{16}$$

where m_p is the proton mass. The fusion power W_f [erg/(cm^3·s)] for DT is given in Eq. (2) with number density–mass density relations from (16), yielding

$$W_{f,DT}\left[\frac{\text{erg}}{\text{cm}^3\cdot\text{s}}\right] = 8.07\times10^{40}\langle\sigma v\rangle_{DT}\,\rho^2 \tag{17}$$

$\langle\sigma v\rangle_{DT}$ is the reactivity of the DT reaction fitted in the domain of ion temperatures $1\text{ keV} < T_i < 100\text{ keV}$ by (Bosch & Hale, 1992)

$$\langle\sigma v\rangle_{DT}\left[\frac{\text{cm}^3}{\text{s}}\right] = 6.4341\times10^{-14}\zeta^{-5/6}\left(\frac{6.661}{T_i{}^{1/3}}\right)^2 \exp\left[-19.983\left(\frac{\zeta}{T_i}\right)^{1/3}\right]$$
$$\zeta = 1 - \frac{15.136T_i + 4.6064T_i{}^2 - 0.10675T_i{}^3}{1000 + 75.189T_i + 13.5T_i{}^2 + 0.01366T_i{}^3}$$
$$T_i \text{ in keV} \tag{18}$$

The electron bremsstrahlung power per unit volume loss, including relativistic corrections, W_B is given by

$$W_B\left[\frac{\text{erg}}{\text{cm}^3\cdot\text{s}}\right] = 8.58\times10^{21}\rho^2 T_e(\text{eV})^{0.5}\left(1 + \frac{2T_e(\text{eV})}{0.511\times10^6}\right) \tag{19}$$

The mechanical expansion power loss is estimated for DT using Eq. (11)

$$W_m\left[\frac{\text{erg}}{\text{cm}^3\cdot\text{s}}\right] = 1.02\times10^{18}[T_e(\text{eV}) + T_i(\text{eV})]^{1.5}\left(\frac{\rho}{R}\right) \tag{20}$$

Substituting the following equations (17) for W_f, (19) for W_B, (9) for W_{he}, and (20) for W_m into Eq. (7) and multiplying by R^2 we get a quadratic inequality in $\rho\cdot R$ as given by Eq. (14) with

$$Y_{DT} \equiv a(T_e, T_i)(\rho R)^2 + b(T_e, T_i)(\rho R) + c(T_e) \geq 0$$
$$a(T_e, T_i) = 8.07\times10^{40}\langle\sigma v\rangle - 8.63\times10^{21}T_e(\text{eV})^{1/2}\left(1 + \frac{2T_e(\text{eV})}{500,000}\right)$$
$$b(T_e, T_i) = -1.02\times10^{18}[T_e(\text{eV}) + T_i(\text{eV})]^{1.5}$$
$$c(T_e) = -\frac{3.11\times10^9 T_e(\text{eV})^{7/2}}{\ln\Lambda} \tag{21}$$

The solution of Eq. (21) with $\langle\sigma v\rangle_{DT}$ from (18) and with $f_\alpha = 1$, $\ln\Lambda = 3.5$ is given in Figure 2. Contours of equal $\rho\cdot R$ as a function of ions and electrons temperatures for DT are displayed. It is seen that for temperatures T_i, T_e in the range 10–50 keV $\rho\cdot R < 1$.

2.1. The pB^{11} Case

$$p + {}^{11}B \rightarrow 3\alpha + 8,700\text{ keV} \tag{22}$$

In this case, due to the ions high temperatures required for fusion and also bremsstrahlung losses of the electrons, the boron to proton number density ratio, ϵ, is usually less than 0.4. In the

https://doi.org/10.1017/S0263034615000701 Published online by Cambridge University Press

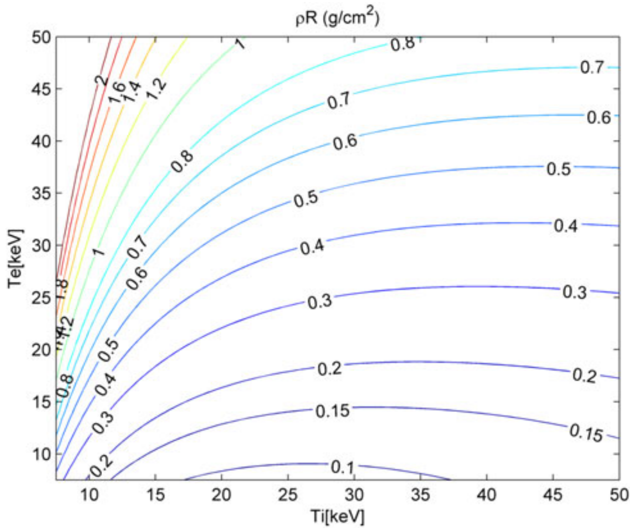

Fig. 2. Contours of equal ρ·*R* as a function of ions and electrons temperatures for DT, obtained from Eqs. (14) and (21).

following terms Eq. (14) is expressed as a function of the ratio ε:

$$\varepsilon = \frac{n_B}{n_p}; \quad n_i = n_B + n_p = (1+\varepsilon)n_p$$
$$\rho = m_i n_i; \quad m_i = \frac{(1+11\varepsilon)}{(1+\varepsilon)} m_p \tag{23}$$

n_B, n_p, and n_i are the appropriate number densities (cm^{-3}) of the boron11, protons, and ions. The electron density n_e is related to the ion density n_i for a neutral plasma with ionization Z_i by

$$n_e = \sum_{k=p,B} Z_k n_k = n_p + 5n_B = \left(\frac{1+5\varepsilon}{1+\varepsilon}\right) n_i$$
$$n_e = \left(\frac{1+5\varepsilon}{1+11\varepsilon}\right)\left(\frac{\rho}{m_p}\right) \tag{24}$$
$$n_i = \left(\frac{1+\varepsilon}{1+11\varepsilon}\right)\left(\frac{\rho}{m_p}\right)$$

The following relations involving ϵ are also important for our calculations

$$\sum_{k=p,B} Z_k^2 n_k = \left(\frac{1+25\varepsilon}{1+\varepsilon}\right) n_i$$
$$\sum_{k=p,B} \frac{Z_k^2 n_k}{m_k} = \left(1 + \frac{25}{11}\varepsilon\right)\frac{1}{(1+\varepsilon)} n_i \tag{25}$$

The fusion power W_f [erg/(cm^3·s)] for pB^{11} is given in Eq. (2) with number density–mass density relations from (24), yielding

$$W_{f,pB11}\left[\frac{erg}{cm^3 \cdot s}\right] = 4.99 \times 10^{42} \frac{\varepsilon \rho^2 <\sigma v>_{pB11}}{(1+11\varepsilon)^2} \tag{26}$$

$<\sigma v>_{pB11}$ is the reactivity of the $p^{11}B$ reaction fitted in the domain of ion temperatures $50\,keV < T_i < 500\,keV$ by (Nevins & Swain, 2000)

$$<\sigma v>_{DT}\left[\frac{cm^3}{s}\right] = 6.4341 \times 10^{-14} \zeta^{-5/6} \left(\frac{6.661}{T_i^{1/3}}\right)^2$$
$$\exp\left[-19.983\left(\frac{\zeta}{T_i}\right)^{1/3}\right] \tag{27}$$
$$\zeta = 1 - \frac{15.136T_i + 4.6064T_i^2 - 0.10675T_i^3}{1000 + 75.189T_i + 13.5T_i^2 + 0.01366T_i^3}$$
T_i in keV

The electron bremsstrahlung power per unit volume loss, including relativistic corrections, W_B is given by

$$W_B\left[\frac{erg}{cm^3 \cdot s}\right] = 5.35 \times 10^{22} \frac{(1+5\varepsilon)(1+25\varepsilon)}{(1+11\varepsilon)^2} \times$$
$$\rho^2 T_e(eV)^{0.5}\left(1 + \frac{2T_e(eV)}{0.511 \times 10^6}\right) \tag{28}$$

The mechanical expansion power loss is estimated for pB^{11} by (Eliezer & Martinez Val, 1998)

$$W_m\left[\frac{erg}{cm^3 \cdot s}\right] = 1.86$$
$$\times 10^{18}\left(\frac{\rho}{R}\right)\left[\frac{(1+5\varepsilon)T_e(eV) + (1+\varepsilon)T_i(eV)}{(1+11\varepsilon)}\right]^{3/2} \tag{29}$$

Substituting the following equations (26) for W_f, (28) for W_B, (9) for W_{he}, and (29) for W_m into Eq. (7) and multiplying by R^2 we get a quadratic inequality in ρ·*R* as given by Eq. (14) with

$$Y_{pB11} \equiv a(T_e, T_i)(\rho R)^2 + b(T_e, T_i)(\rho R) + c(T_e) \geq 0$$
$$a(T_e, T_i) = f_\alpha 4.99 \times 10^{42} \frac{\varepsilon <\sigma v>_{pB11}}{(1+11\varepsilon)^2}$$
$$- 5.35 \times 10^{22} \frac{(1+5\varepsilon)(1+25\varepsilon)}{(1+11\varepsilon)^2}$$
$$\times T_e(eV)^{0.5}\left(1 + \frac{2T_e(eV)}{0.511 \times 10^6}\right)$$
$$b(T_e, T_i) = -1.86 \times 10^{18}\left[\frac{(1+5\varepsilon)T_e(eV) + (1+\varepsilon)T_i(eV)}{(1+11\varepsilon)}\right]^{3/2}$$
$$c(T_e) = -\frac{3.11 \times 10^9 T_e(eV)^{7/2}}{\ln \Lambda} \tag{30}$$

The solution of Eq. (30) and $<\sigma v>_{pB11}$ from (27) with $f_\alpha = 1$, $\ln\Lambda = 3.5$, and $\varepsilon = 0.33$, is given in Figure 3. It is seen that temperature ranges where Eq. (30) has real solutions $\rho \cdot R < 20$ are 100–600 keV for the ions and 10–100 keV for the electrons. Moreover, the values of ρ·R are larger by about two orders of magnitude than for DT, requiring larger pre-compression and igniter size, and as it is shown below; larger energy laser.

https://doi.org/10.1017/S0263034615000701 Published online by Cambridge University Press

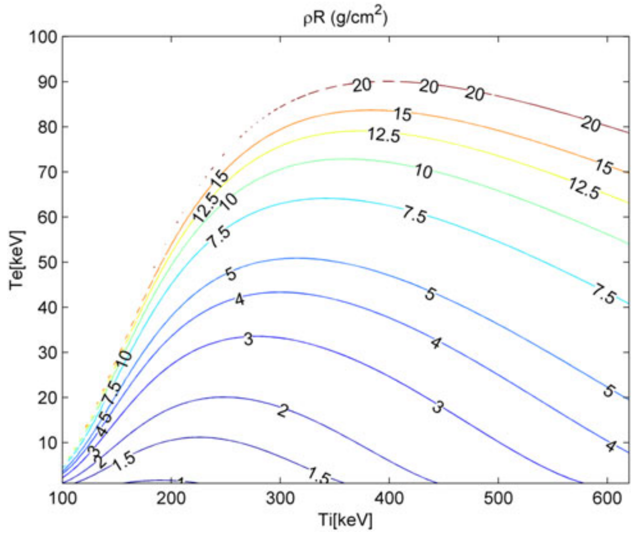

Fig. 3. Contours of equal ρ·R as a function of ions and electrons temperatures for pB11, obtained from Eqs. (14) and (30).

3. THE IGNITER PERFORMANCE DRIVEN BY LASER INDUCED TWO TEMPERATURES SHOCK WAVES

As described in Section 1, in the framework of the piston model, a shock wave is generated in the target, with different ions and electrons temperatures. Following Chu (1972) and Eliezer and Martinez-Val (1998), the igniter performance can be analyzed by an energy balance, dependent on the ions and electrons temperatures:

$$\begin{aligned} &\left(\frac{3}{2}\right)\frac{d}{dt}(n_e k_B T_e) = \eta_d W_d + W_{ie} - W_B + f_\alpha \eta_f W_f \\ &\left(\frac{3}{2}\right)\frac{d}{dt}(n_i k_B T_i) = (1-\eta_d) W_d - W_{ie} + f_\alpha (1-\eta_f) W_f \end{aligned} \tag{31}$$

A schematic view of this two temperatures shock model is given in Figure 4. Note that during the time the shock wave is driven by the laser-piston the heat wave and mechanical losses do not exist. k_B is the Boltzmann's constant. W_d [erg/(cm^3·s)] is the power density deposited by the driver (induced by the laser-piston), η_d is the fraction of the driver energy deposited in the electrons inside the shocked volume, $(1-\eta_d)$ gives the fraction of the driver energy deposited in the ions inside the shocked volume.

The deposition power density W_d is dependent on the laser intensity I_L and pulse time duration τ_L and on the shock compression $\kappa = \rho/\rho_0$ (see Appendix A):

$$I_L\left[\frac{W}{cm^2}\right] = 4\times 10^3 \frac{W_d\left[\frac{erg}{cm^3\cdot s}\right]\tau_L[s]}{\kappa} \tag{32}$$

The relation between the deposition power density and the laser parameters, as well as the particle u_p and shock u_s velocities are obtained from the Hugoniot–Rankine equations and presented in Appendix C. The size of the igniter is determined by the laser and the fuel parameters. The igniter is modeled as a cylinder with length $R = l_s$, the shock dimension, defined in Eq. (4) and diameter $2R_L = 3l_s$, larger than the shock dimension to justify1D approximation.

As described in Section 2, the shock dimension is used in the calculation of f_α, the fraction of the α-particles (created in the DT or pB^{11} fusion) energy deposited inside the shocked volume.

Assuming that λ_i and λ_e are the appropriate mean free paths of the ions and electrons in plasma, one gets for η_d

$$\begin{aligned} &\eta_d = \frac{\lambda_i}{\lambda_i + \lambda_e} \\ &\lambda_i[cm] = \left(\frac{3\times 10^{23}}{n_i}\right)\left(\frac{m_p}{m_i}\right)E_i[MeV] \\ &\lambda_e[cm] = \left(\frac{5\times 10^{22}}{n_e \ln\Lambda}\right)T_e[keV]^{3/2}E_i[MeV] \\ &E_i = \frac{1}{2}m_i u_p^2 = 1250(MeV)\left(\frac{u_p}{c}\right)^2 \end{aligned} \tag{33}$$

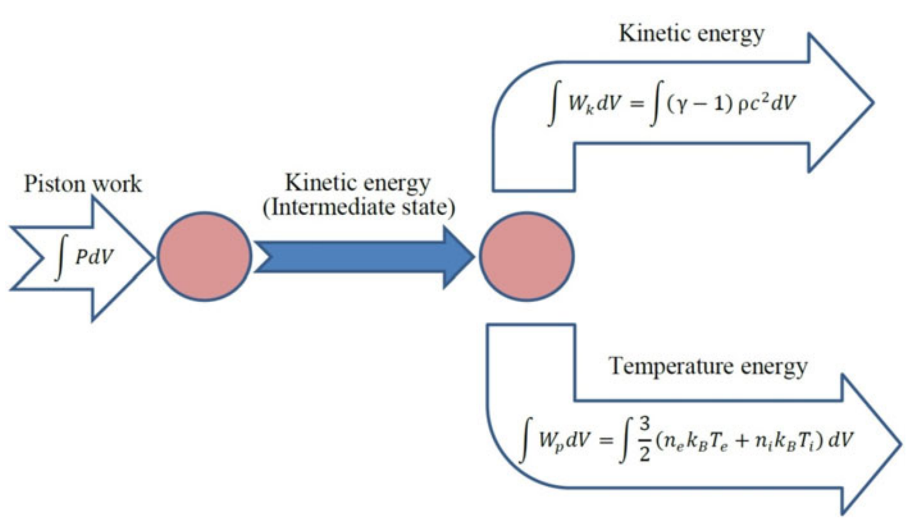

Fig. 4. A schematic picture of the two temperature shock wave creation.

https://doi.org/10.1017/S0263034615000701 Published online by Cambridge University Press

It is important to mention that although λ_i and λ_e can in general be larger than the time dependent shocked domain $u_p \cdot t$, the charged particles that heat the shocked area have a velocity u_p and therefore are not moving faster than the shock wave since $u_s > u_p$. Thus the shock wave moves into a cold domain not yet heated by the driver energy.

W_{ie} [erg/(cm^3·s)] is the ion–electron exchange power density given by

$$W_{ie}\left[\frac{\text{erg}}{\text{cm}^3 \cdot \text{s}}\right] = 2.70 \times 10^{-22} n_e \left(\frac{T_i(E) - T_e(\text{keV})}{T_e(\text{keV})^{1.5}}\right) \sum_k \frac{Z_k{}^2 n_k}{m_k} \ln \Lambda_{ek} \tag{34}$$

W_B [erg/(cm^3·s)], the electron bremsstrahlung power density losses and W_f [erg/(cm^3·s)], the fusion power density created in the shocked volume, were defined in Section 2. η_f is the energy fraction that is deposited in the electrons by the α-particles created in the fusion under consideration and $(1-\eta_f)$ describes the energy fraction that is deposited in the ions by these α-particles. The function η_f for DT fusion was taken from Chu (1972):

$$\eta_f = \frac{32}{32 + T_e(\text{keV})} \tag{35}$$

For proton–boron fusion, the function η_f was taken from Eliezer and Martinez-Val (1998):

$$\eta_f = \frac{150}{150 + T_e^{1.5}(\text{keV})} \tag{36}$$

The time dependent temperatures equations are coupled to equations for the number densities of the ions species. For DT these equations read:

$$\frac{dn_D}{dt} = \frac{dn_T}{dt} = -\frac{dn_\alpha}{dt} = -n_D n_T <\sigma v>_{DT} \tag{37}$$

where, n_D, n_T, and n_α are number densities of the deuterons, protons, and α-particles.

For proton–boron fusion the time evolution of the number densities of the ions species is:

$$\begin{aligned} \frac{dn_p}{dt} &= \frac{dn_B}{dt} = -n_p n_B <\sigma v>_{pB} \\ \frac{dn_\alpha}{dt} &= 3 n_p n_B <\sigma v>_{pB} \end{aligned} \tag{38}$$

Given the laser and the fuel parameters, the ions and the electrons temperatures and densities time evolution can be obtained.

In the scheme of shock fast ignition considered here, the product $\rho \cdot R = \rho \cdot l_s$ is determined by the laser and fuel parameters. Following the criterion described in Section 2, ignition occurs if at some time t_{ig} during the laser pulse duration, temperatures values are obtained such that a solution of energy balance (14) exists with $T_i(t_{ig})$, $T_e(t_{ig})$. In the framework of the model presented here, if such a solution exists, after time t_{ig}, the surrounding fuel burns due to the released fusion energy in the igniter. Therefore, the product $\rho \cdot R[T_i(t), T_e(t)]$ is solved from Eq. (14) and ignition occurs if:

$$\rho \cdot R\left[T_i(t_{ig}),\ T_e(t_{ig})\right] < \rho \cdot l_s \tag{39}$$

4. ELECTRON AND ION TEMPERATURES CALCULATIONS FOR DT AND PB^{11}

In this section solutions of the two temperatures shock model for DT and pB^{11} cases are presented, for laser parameters for which ignition is obtained during the laser pulse.

Figures 5–7 display the results of the two temperatures model given in Eqs. (31, 38) for DT pre-compressed to density $\rho_0 = 600$ g/cm^3. The fast ignition shock generated by irradiation with laser intensity of 7.5×10^{22} W/cm^2, 1 ps pulse duration, and energy 3.67 kJ induces a compression of $\kappa = 4$. The laser energy density deposition in this case is $W_d = 7.5 \times 10^{31}$ erg/cm^{3}s and the shock length, the igniter dimension in our model, is $l_s = 0.833$ μm. Therefore, in this case $\rho \cdot R = 0.2$ g/cm^2. For ignition, it is required that due to the shock wave energy deposition, to reach temperatures values where Eq. (14) has a solution $\rho\ R \le 0.2$ g/cm^2. The electrons and ions temperatures, $T_e(t)$, $T_i(t)$ as a function of time, and $\rho \cdot R$, obtained by solving Eq. (14) given $T_e(t)$, $T_i(t)$ are shown in Figure 5. It is seen that the ion temperature increase to about 68 keV and the electron temperature reaches 42 keV by the end of the laser pulse (Fig. 5b). There is no real solution of Eq. (14) for the product $\rho \cdot R$ for times less than about 0.1 ps (Fig. 5b). As the temperatures rise, Eq. (14) has real solutions, decreasing to $\rho \cdot R = 0.2$ g/cm^2 at about 0.3 ps, when the ions and electrons temperatures are slightly higher than 10 keV and ignition is set on. At this time fusion energy deposition rises and exceeds the shock wave energy deposition. The different terms in Eq. (31), deposition, fusion, radiation losses, and electron–ion exchange energy densities, as a function of time are given in Figure 6. The fraction of absorbed α-particles in the hot spot as a function of time is described in Figure 7. It is seen that as the time evolves and the temperatures increase, a larger fraction of α-particles leave the igniter region heating up the surroundings.

Proton–boron fusion requires higher temperatures to reach ignition compared with DT, mainly due to the higher radiation losses, implying larger size and more dense igniters. These constrains require larger laser energies, making the shock based fast ignition scheme presented here for pB^{11} fusion impracticable. The temperatures and the ρ·R product as a function of time for a pB^{11} case that may reach ignition according to the criterion considered here are displayed in Figure 8. However, in this case the igniter size is larger, $l_s = 4.32$ μm, the pre-compressed fuel density is $\rho_0 = 4800$ g/cm^3, and the product required for ignition is $\rho \cdot R =$

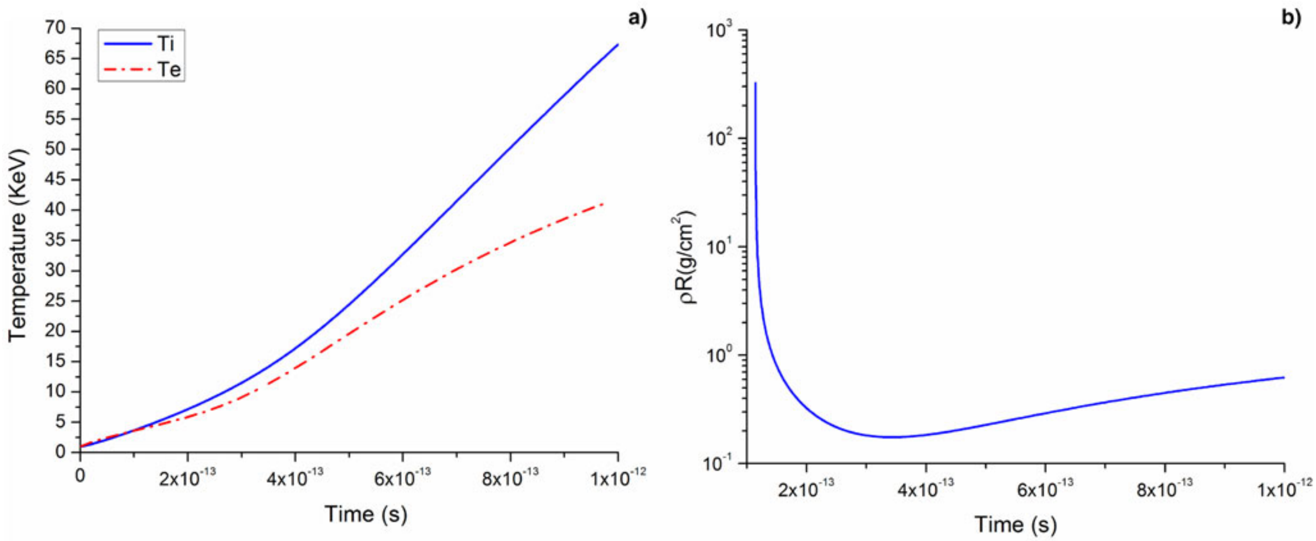

Fig. 5. (a) Electrons T_e and protons T_i temperatures as a function of time for a DT case satisfying the ignition criterion, (b) $\rho{\cdot}R$ as function of time obtained by solving Eqs. (14) and (21).

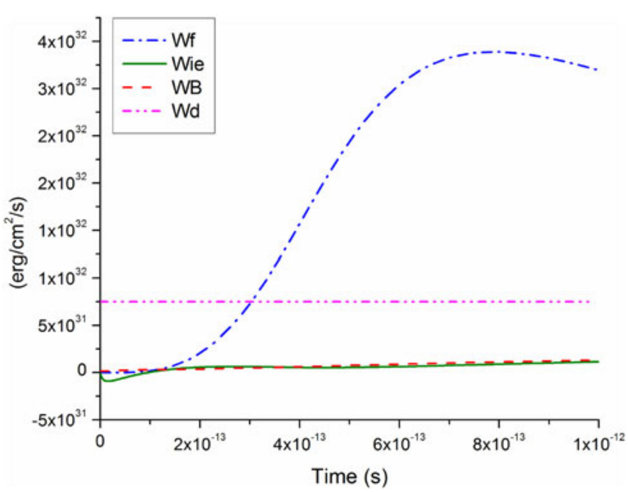

Fig. 6. Various energy power density terms in Eq. (31) as a function of time for the DT case displayed in Figure 5.

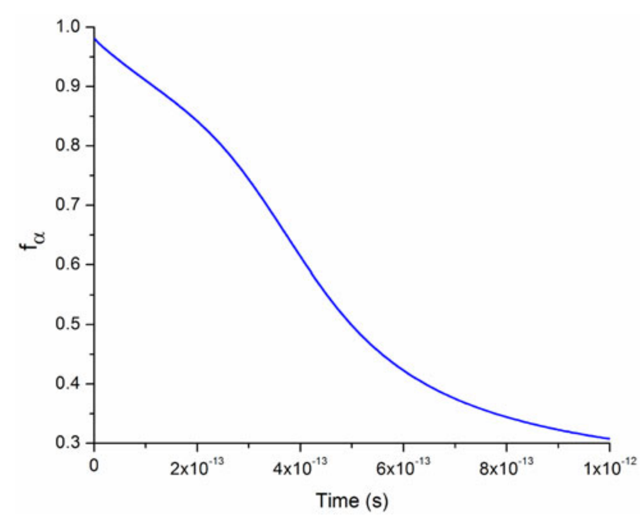

Fig. 7. The fusion energy fraction deposited in the igniter domain, defined in Eq. (3) for the DT case described in Figure 5.

$8.3\ g/cm^2$. Therefore, the laser pulse generating the fast shock ignition should have an intensity of $1.61 \times 10^{25}\ W/cm^2$, pulse duration of 1 ps, and energy of 21 MJ. The laser power of such system is in the exawatt range. Although such super-laser system is planned at University of Texas, it is still years away from actual development.

5. SUMMARY AND DISCUSSION

In this paper a general fuel ignition criterion for two temperatures plasma is presented. This criterion was considered for DT and pB^{11} pre-compressed plasma. Two temperatures plasma are important for schemes of nuclear fast ignition fusion, based on short pulse lasers. Here we applied the ignition criterion to a fast ignition scheme based on intense short pulse laser generated shock wave. The ignition criterion stems from energy balance between fusion energy and radiation, expansion and heat conduction losses, and is described by a surface in the 3D space defined by the electron and ion temperatures T_e, T_i, and the plasma density times the hot spot dimension, $\rho{\cdot}R$. For appropriate fusion ion temperatures, namely T_i larger than 10 keV for DT, and T_i larger than 150 keV for pB^{11}, the value of $\rho{\cdot}R$ required for ignition for pB^{11} is larger by a factor of 50 or more than for DT, depending on the electron temperature. Furthermore, following the ignition criterion described here, pB11 fusion is practically not possible if the electron and ion temperatures are equal, see also Kouhi *et al*. (2011). To eliminate these problems for pB11 fusion, application of non-thermal conversion of the laser energy by picosecond laser pulses to ultrahigh acceleration of plasma blocks (Chu, 1972) to initiate the fusion

https://doi.org/10.1017/S0263034615000701 Published online by Cambridge University Press

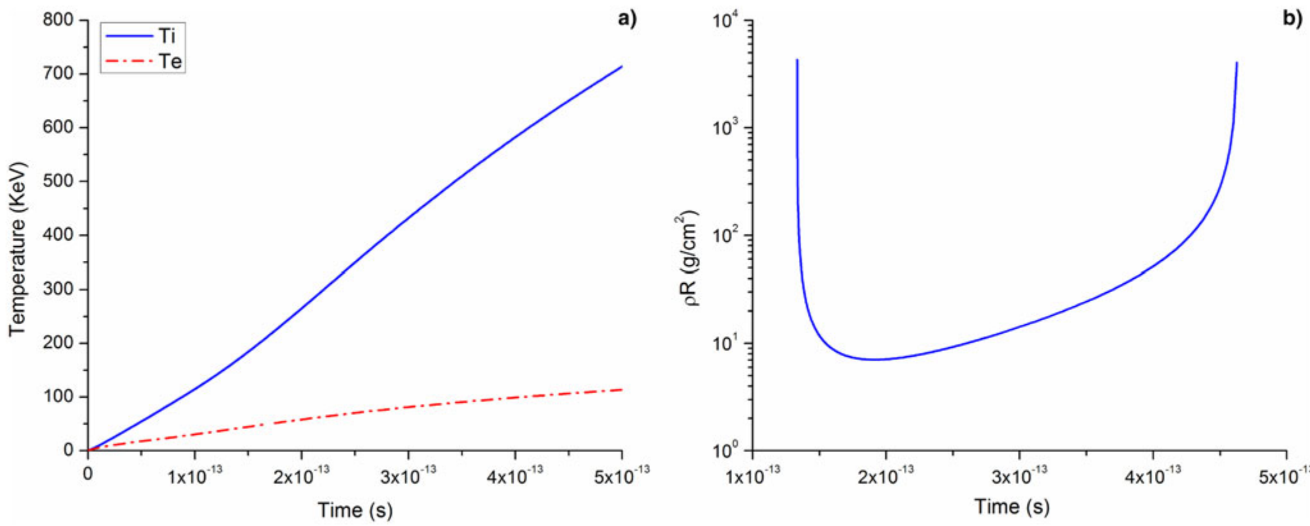

Fig. 8. (a) Electrons T_e and protons T_i temperatures as a function of time for a pB^{11} case satisfying the ignition criterion, (b) $\rho \cdot R$ as function of time obtained by solving Eqs (14) and (30).

reaction in solid density DT or pB11 fuel (Lalousis *et al.*, 2013; 2014; Hora *et al.*, 2015).

Our suggested model for fast ignition based on two temperature laser induced shock wave in the intermediate domain between relativistic and non-relativistic shock waves is summarized. The size of the hot spot is dependent on the laser pulse intensity and time duration. Scaling laws between ρ R and the laser and fuel parameters are presented in Appendix A.

The laser parameters for fast ignition for DT and pB^{11} are calculated. For DT case one needs 3 kJ energy, 1 ps laser pulse duration to ignite a pre-compressed target at about 600 g/cm^3. These laser parameters are of the same order as other fast ignition schemes (Naumova *et al.*, 2009). However, this scheme is not practical for pB^{11} ignition since it requires a laser with more than three orders of magnitude energy for the same pulse duration.

REFERENCES

Atzeni, S. & Meyer-Ter-Vehn, J. (2004). *The Physics of Inertial Fusion*. Oxford: Claredon Press.

Basov, N.G., Guskov, S.Y. & Feoktistov, L.P. (1992). Thermonuclear gain of ICF targets with direct heating of the ignitor. *J. Soviet Laser Res*. **13**, 396–399.

Betti, R., Zhou, C.D., Anderson, K.S., Perkins, L.J., Theobald, W. & Sokolov, A.A. (2007). Shock ignition of thermonuclear fuel with high areal density. *Phys. Rev. Lett*. **98**, 155001/1–4.

Bosch, H.S. & Hale, G.M. (1992). Improved formulas for fusion cross-sections and thermal reactivities. *Nucl. Fusion* **32**, 611–631.

Cicchitelli, L., Hora, H. & Postle, R. (1990). Longitudinal field components of laser beams in vacuum. *Phys. Rev. A* **41**, 3727–3732.

Chu, M.S. (1972). Thermonuclear reaction waves at high densities. *Phys. Fluids* **15**, 413–422.

Eliezer, S. (2002). *The Interaction of High-Power Lasers with Plasmas*. Boca Raton, Florida: CRC press.

Eliezer, S. (2012). Relativistic acceleration of micro-foils with prospects for fast ignition. *Laser Part. Beams* **30**, 225–232.

Eliezer, S. (2013). Shock waves and Equations of state related to laser–plasma interaction. In *Laser–Plasma Interactions and Applications*, 68th Scottish Universities Summer School in Physics, (McKenna, P., Neely, D., Bingham, R. and Jaroszynski, D.A., Eds.), Heidelberg: Springer Publication, pp. 49–78.

Eliezer, S., Hora, H., Kolka, E., Green, F. & Szichman, H. (1995). How double layers accelerate charged particles. *Laser Part. Beams* **13**, 441–447.

Eliezer, S. & Martinez Val, J.M. (1998). Proton-boron 11 fusion reactions induced by heat-detonation burning waves. *Laser Part. Beams* **16**, 581–598.

Eliezer, S. & Martinez Val, J.M. (2011). The comeback of shock waves in inertial fusion energy. *Laser Part. Beams* **29**, 175–181.

Eliezer, S., Nissim, N., Pinhasi, V.S., Raicher, E. & Martinez Val, J.M. (2014a). Ultrafast ignition with relativistic shock waves induced by high power lasers. *High Power Laser Sci. Eng*. **2**, 10. doi: 10.1017/hpl.2014.24

Eliezer, S., Nissim, N., Raicher, E. & Martinez Val, J.M. (2014b). Relativistic shock waves induced by ultra-high laser pressure. *Laser Part. Beams* **32**, 243–251.

Eliezer, S., Nissim, N., Martinez Val, J.M., Mima, K. & Hora, H. (2014c). Double layer acceleration by laser radiation. *Laser Part. Beams* **32**, 211–216.

Esirkepov, T., Borghesi, M., Bulanov, S.V., Mourou, G. & Tajima, T. (2004). Highly efficient relativistic ion generation in the laser-piston regime. *Phys. Rev. Lett*. **92**, 175003/1–4.

Fortov, V.E. & Lomonosov, I.V. (2010). Shock waves and equations of state of matter. *Shock Waves* **20**, 53–71.

Guskov, S.Y. (2013). Fast ignition of inertial confinement fusion targets. *Plasma Phys. Rep*. **39**, 1–50.

Guskov, S.Y., Krokhin, O.N. & Rozanov, V.B. (1976). Similarity solution of thermonuclear burn wave with electron and α conductivities. *Nucl. Fusion* **16**, 957–962.

Guskov, S.Y. & Rozanov, V.B. (1993). Ignition and burn propagation in ICF targets. In *Nuclear Fusion by Inertial Confinement: A comprehensive Treatise*. (Velarde, G., Ronen, Y. & Martinez Val, J.M., Eds.), Baton Roca, Florida: CRC press, pp. 293–320.

Hora, H. (1991). *Plasmas of High Temperatures and Density*. Heidelberg: Springer.

Hora, H., Lalousis, P. & Eliezer, S. (1984). Analysis of the inverted double layers produced by nonlinear forces in laser produced plasmas. *Phys. Rev Lett*. **53**, 1650–1653.

Hora, H., Lalousis, P., Giuffrida, L., Margarone, D., Korn, G., Eliezer, S., Miley, G., Moustaizis, S. & Mourou, G. (2015). Petawatt laser pulses for proton-boron high gain fusion with avalanche reactions excluding problems of nuclear radiation. *Proc. SPIE* 9515, 951518. doi: 10.1117/12.2181943.

Hora, H., Lalousis, P. & Moustaizis, S. (2014). Fiber ICAN laser with exawatt picosecond pulses for fusion without nuclear radiation problems. *Laser Part. Beams* **32**, 63–68.

Kouhi, M., Ghoraneviss, M., Malekynia, B., Hora, B., Miley, G.H., Sari, A.H., Azizi, N., & Razavipour, S.S. (2011). Resonance effect for strong increase of fusion gains at thermal compression for volume ignition of Hydrogen Boron-11. *Laser Part. Beams* **29**, 125–134.

Lalousis, P. & Hora, H. (1983). First direct electron and ion fluid computation of high electrostatic fields in dense inhomogeneous plasmas with subsequent nonlinear laser interaction. *Laser Part. Beams* **1**, 283–304.

Lalousis, P., Foldes, I.B. & Hora, H. (2012). Ultra-high acceleration of plasma by picosecond terawatt laser pulses for fast ignition of fusion. *Laser Part. Beams* **30**, 233–242.

Lalousis, P., Hora, H., Eliezer, S., Martinez Val, J.M., Moustaizis, S., Miley, G.H. & Mourou, G. (2013). Shock Mechanisms by ultra-high laser accelerated plasma blocks in solid density targets for fusion. *Phys. Lett.* A **377**, 885.

Lalousis, P., Hora, H. & Moustaizis, S. (2014). Optimized boron fusion with magnetic trapping by laser driven plasma block initiation at nonlinear forced driven ultrahigh acceleration. *Laser Part. Beams* **32**, 409–411.

Landau, L.D. & Lifshitz, E.M. (1987). *Fluid Mechanics*, 2nd edn. Oxford: Pergamon Press.

Lindl, J.D. (1988). Physics of ignition for ICF capsules. In *International School of Plasma Physics Piero Caldirola: Inertial Confinement Fusion*. (Caruso, A. & Sindoni, E., Eds.), Bologna: Editrice Compositori, pp. 617.

Naumova, N., Schlegel, T., Tikhonchuk, V.T., Labaune, C., Sokolov, I.V. & Mourou, G. (2009). Hole boring in a DT pellet and fast ion ignition with ultra-intense laser pulses. *Phys. Rev. Lett.* **102**, 025002/1–4.

Nevins, W.M. & Swain, C. (2000). The thermonuclear fusion coefficient for p-^{11}B reactions. *Nucl. Fusion* **40**, 865–872.

Nuckolls, J.H., Wood, L., Thiessen, A. & Zimmermann, G.B. (1972). Laser compression of matter to super-high densities: Thermonuclear applications. *Nature* **239**, 139–142.

Rozanov, V.B., Verdon, C.P., Decroisette, M., Guskov, S.Y., Lindl, J.D., Nishihara, K. & Takabe, H. (1995). *Inertial Confinement Target Physics. Energy from Inertial Fusion* Vienna: International Atomic Energy Agency, pp. 21–69.

Tabak, M., Hammer, J., Glinsky, M.E., Kruer, W.L., Wilks, S.C., Woodworth, J., Campbell, E.M., Perry, M.D. & Mason, R.S. (1994). Ignition and high gain with ultra-powerful lasers. *Phys. Plasmas* **1**, 1626–1634.

Takabe, H., Mima, K. & Nakai, S. (1989). Requirement of uniformity for fuel ignition and uniformity in high neutron yield implosion. *Laser Part. Beams* **7**, 175–188.

Taub, A.H. (1948). Relativistic Rankine–Hugoniot equations. *Phys. Rev*. **74**, 328–334.

Velarde, G. & Carpintero-Santamaria, N. eds. (2007). *Inertial Confinement Nuclear Fusion: A Historical Approach by its Pioneers*. UK: Foxwell and Davies Pub.

Zeldovich, Y.B. & Raizer, Y.P. (1966). *Physics of Shock Waves and High Temperature Hydrodynamic Phenomena*. New York: Academic Press Publications.

APPENDIX

APPENDIX A: RELATIVISTIC AND NON-RELATIVISTIC SHOCK WAVE RANKINE–HUGONIOT EQUATIONS

The relativistic shock wave Hugoniot equations in the laboratory frame of reference are given by the following equations

$$\begin{aligned}
&\text{(i)}\ \frac{u_{p1}}{c} = \sqrt{\frac{(P_1 - P_0)(e_1 - e_0)}{(e_0 + P_1)(e_1 + P_0)}}\\
&\text{(ii)}\ \frac{u_s}{c} = \sqrt{\frac{(P_1 - P_0)(e_1 + P_0)}{(e_1 - e_0)(e_0 + P_1)}}\\
&\text{(iii)}\ \frac{(e_1 + P_1)^2}{\rho_1{}^2} - \frac{(e_0 + P_0)^2}{\rho_0{}^2}\\
&\quad = (P_1 - P_0)\left[\frac{(e_0 + P_0)}{\rho_0{}^2} + \frac{(e_1 + P_1)}{\rho_1{}^2}\right]
\end{aligned} \tag{A1}$$

P, e, and ρ are the pressure, energy density and mass density accordingly, the subscripts 0 and 1 denote the domains before and after the shock arrival, u_s is the shock wave velocity and u_{p1} is the particle flow velocity in the laboratory frame of reference and *c* is the speed of light. We have assumed that in the laboratory the target is initially at rest, $u_{p0} = 0$. The EOS taken here in order to calculate the shock wave parameters is the ideal gas EOS

$$e_j = \rho_j c^2 + \frac{P_j}{\Gamma - 1};\ j = 0, 1. \tag{A2}$$

where Γ is the specific heat ratio. We have to solve Eqs (A1) and (A2) together with our piston model equation (Esirkepov *et al*., 2004; Eliezer *et al*., 2014b)

$$P_1 = \frac{2I_L}{c}\left(\frac{1-\beta}{1+\beta}\right);\ \beta \equiv \frac{u_{p1}}{c} \tag{A3}$$

We have five equations given in (A1), (A2), and (A3) with five unknowns: u_s, u_{p1}, P_1, ρ_1, and e_1 assuming that we know I_L, ρ_0, P_0, e_0, and Γ. We take ideal gas EOS with $\Gamma = 5/3$. The calculations are conveniently done in the dimensionless units defined by

$$\Pi_L \equiv \frac{I_L}{\rho_0 c^3}; \kappa \equiv \frac{\rho_1}{\rho_0}; \kappa_0 \equiv \frac{\Gamma+1}{\Gamma-1}; \Pi = \frac{P_1}{\rho_0 c^2}; \Pi_0 = \frac{P_0}{\rho_0 c^2} \quad \text{(A4)}$$

It is important to emphasize that if we take $P_0 = 0$ then we get only the $\kappa > 4$ solutions (Eliezer *et al.*, 2014a), therefore in order to see the behavior at the transition between relativistic and non-relativistic domain one has to take $P_0 \neq 0$! In our numerical estimations we take $P_0 = 1$ bar $= 10^6$ in cgs units. For example, the Hugoniot Eq. (A1) together with the EOS Eq. (A2) yield

$$\frac{P_0}{P_1} = \frac{\Pi_0}{\Pi} = \mathbf{0} \Rightarrow \begin{cases} \Pi = -B(\Pi_0 = 0) = \dfrac{(\Gamma-1)^2}{\Gamma}\kappa(\kappa-\kappa_0) \\ \kappa \equiv \dfrac{\rho_1}{\rho_0} \geq \kappa_0 \end{cases} \quad \text{(A5)}$$

$$\begin{aligned} &\frac{P_0}{P_1} = \frac{\Pi_0}{\Pi} \neq \mathbf{0} \Rightarrow \begin{cases} \Pi^2 + B\Pi + C = 0 \\ \kappa \equiv \dfrac{\rho_1}{\rho_0} \geq 1 \end{cases} \\ &\Pi = \left(\frac{1}{2}\right)\left(-B \pm \sqrt{B^2 - 4C}\right) \\ &B = \frac{(\Gamma-1)^2}{\Gamma}(\kappa_0\kappa - \kappa^2) + \Pi_0(\Gamma-1)(1-\kappa^2) \\ &C = \frac{(\Gamma-1)^2}{\Gamma}(\kappa - \kappa_0\kappa^2)\,\Pi_0 - \kappa^2{\Pi_0}^2 \end{aligned} \quad \text{(A6)}$$

The compression κ as a function of the dimensionless pressure $\Pi = P/(\rho_0 c^2)$ is given in Figure 9 for $\kappa_0 = 4$ ($\Gamma = 5/3$). Although P_0/P_1 is extremely small one cannot neglect it in the very near vicinity of κ_0 and in this domain one has to solve numerically Eq. (A6). Furthermore, in order to see the transition between the relativistic and non-relativistic approximation one has to solve the relativistic equations in order to see the transition effects like the one shown in Figure 9.

For convenience we write the non-relativistic Hugoniot equations for the ideal gas EOS:

$$\begin{aligned} &\text{(i) } u_{p1} = [P_1 - P_0]^{1/2}\left(\frac{1}{\rho_0} - \frac{1}{\rho_1}\right)^{1/2} \\ &\text{(ii) } u_s = \left(\frac{1}{\rho_0}\right)\frac{[P_1 - P_0]^{1/2}}{\left(\dfrac{1}{\rho_0} - \dfrac{1}{\rho_1}\right)^{1/2}} \\ &\text{(iii) } E_1 - E_0 = \left(\frac{1}{2}\right)[P_1 + P_0]\left(\frac{1}{\rho_0} - \frac{1}{\rho_1}\right) \\ &\left.\begin{matrix}\text{(iv)} \\ \text{(v)}\end{matrix}\right\} E_j = \left(\frac{1}{\Gamma - 1}\right)\left(\frac{P_j}{\rho_j}\right) \text{ for } j = 0, 1 \end{aligned} \quad \text{(A7)}$$

These equations are obtained from the relativistic Eq. (A1) by using $e = \rho c^2 + \rho E$, P, and ρE are much smaller than ρc^2 and $u/c \ll 1$ where u stands for the velocities under consideration.

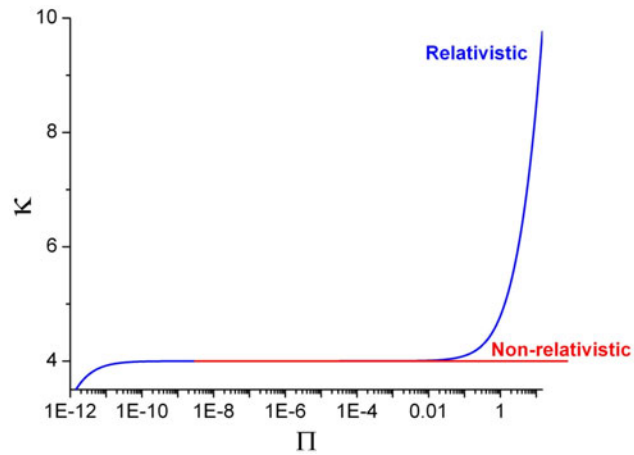

Fig. 9. Compressibility as a function of the normalized shock pressure.

In the transition domain, between relativistic and non-relativistic shock waves we have (see Fig. 2)

$$10^{-9} \leq \Pi \leq 10^{-3} \Leftrightarrow \kappa = \frac{\rho}{\rho_0} = 4.00 \quad \text{(A8)}$$

In the domain defined by Eq. (A8) we have $u_s/c \ll 1$ and $u_p/c \ll 1$ and the non-relativistic Eq. (A7) are satisfied. Therefore in this transition domain the particle and shock wave velocities and the dimensionless shock wave pressure Π, normalized by $\rho_0 c^2$, are obtained from the non-relativistic equations, namely

$$\begin{aligned} &\frac{u_p}{c} = \sqrt{\frac{3}{4}\Pi}; \frac{u_s}{c} = \sqrt{\frac{4}{3}\Pi} \\ &\Pi = \left(\frac{u_s}{c}\right)\left(\frac{u_p}{c}\right) \\ &\frac{u_s}{c} - \left(\frac{u_p}{c}\right) = \frac{1}{3}\left(\frac{u_p}{c}\right) \end{aligned} \quad \text{(A9)}$$

For the intermediate domain, relativistic to non-relativistic case where $\kappa = 4$, the shock wave fast ignition driver W_d is given by

$$W_d\left[\frac{\text{erg}}{\text{cm}^3 \cdot \text{s}}\right] = \frac{1}{2}\left(\frac{\kappa\rho_0 {u_p}^2}{\tau_L}\right) \quad \text{(A10)}$$

This relation is further elaborated in Appendix C.

Using Eqs (A9, A10) we get

$$\begin{aligned} &\frac{u_p}{c} = \sqrt{\frac{2w_d\tau_L}{\kappa\rho_0 c^2}} \\ &\Pi = \left(\frac{8}{3}\right)\frac{w_d\tau_L}{\kappa\rho_0 c^2} \end{aligned} \quad \text{(A11)}$$

In this domain we also have the following relation between

https://doi.org/10.1017/S0263034615000701 Published online by Cambridge University Press

the dimensionless laser irradiance and the shock pressure

$$\frac{I_L}{\rho_0 c^3} \equiv \Pi_L \simeq \frac{\Pi}{2} \tag{A12}$$

From Eqs (A9–A12) we have

$$I_L\left[\frac{W}{\mathrm{cm}^2}\right] = 4\times 10^3 \frac{W_d\left[\frac{\mathrm{erg}}{\mathrm{cm}^3\cdot \mathrm{s}}\right]\tau_L[\mathrm{s}]}{\kappa} \tag{A13}$$

The shock wave length domain $l_s = R$ is related to the deposition power density by:

$$\begin{aligned} \ell_s &= (u_s - u_p)\tau_L = \frac{u_p \tau_L}{3} = \frac{\tau_L}{3}\sqrt{\frac{2W_d\tau_L}{\kappa\rho_0}} \\ \rho R &= \rho\ell_s = \sqrt{\frac{2W_d\kappa\rho_0{\tau_L}^3}{9}} \end{aligned} \tag{A14}$$

The laser cross-section area S is given by

$$\begin{aligned} R_L &= \frac{3}{2}\ell_s \\ S &= \pi {R_L}^2 = \frac{9\pi}{4}{\ell_s}^2 = \frac{\pi}{2}\frac{W_d{\tau_L}^3}{\kappa\rho_0} \end{aligned} \tag{A15}$$

Therefore the laser energy W_L and the irradiance I_L have the following scaling law

$$\begin{aligned} W_L[J] &= I_L\left[\frac{W}{\mathrm{cm}^2}\right]\tau_L[s]S[\mathrm{cm}^2] \\ W_L[J] &= 2\pi\times 10^3 \frac{W_d\left[\frac{\mathrm{erg}}{\mathrm{cm}^3\cdot \mathrm{s}}\right]^2 \tau_L[s]^5}{\kappa^2\rho_0} \\ I_L\left[\frac{W}{\mathrm{cm}^2}\right] &= \frac{4\times 10^3 W_d\tau_L}{\kappa} \end{aligned} \tag{A16}$$

The density times hot spot dimension scaling law is:

$$\rho R = \kappa\rho_0\ell_s \propto {W_d}^{0.5}\kappa^{0.5}{\rho_0}^{0.5}{\tau_L}^{1.5} \tag{A17}$$

Finally, for a constant ρ·R the relevant scaling laws are

$$\begin{aligned} W_L &\propto \frac{1}{\tau_L{\rho_0}^3\kappa^3} \\ I_L &\propto \frac{1}{{\tau_L}^2\rho_0\kappa^2} \end{aligned} \tag{A18}$$

For example, the following table summarizes the dimensionless numerical values of our laser and shock wave parameters

Table A1. *Shock wave parameters relevant for fast ignition*

Π_L	Π	κ	u_p/c	u_s/c
1.90×10^{-5}	3.8×10^{-5}	4.00	0.0053	0.0071
2.99×10^{-5}	5.9×10^{-5}	4.00	0.0067	0.0089
6.65×10^{-5}	1.33×10^{-4}	4.00	0.010	0.013
1.00×10^{-4}	2.7×10^{-4}	4.00	0.015	0.020

For example, if the pre-compressed target has a mass density of 250 $\mathrm{g/cm^3}$ and the laser pulse duration is 1 ps then for the dimensionless laser irradiance of $\Pi_L = 6.65\times 10^{-5}$ we get

$$\begin{aligned} &\Pi_L = 6.65\times 10^{-5};\ \tau_L = 1\,ps; \\ &\rho_0 = 250\left[\frac{\mathrm{g}}{\mathrm{cm}^3}\right] \Rightarrow \rho = \kappa\rho_0 = 10^3\left[\frac{\mathrm{g}}{\mathrm{cm}^3}\right] \\ &I_L = \rho_0 c^3\Pi_L = 4.5\times 10^{22}\left[\frac{W}{\mathrm{cm}^2}\right] \\ &\ell_s = (u_s - u_p)\tau_L \simeq 1\ \mu\mathrm{m}; \\ &S = \pi {R_L}^2 = \pi(1.5\ell_s)^2 = 7.04\times 10^{-8}[\mathrm{cm}^2] \\ &W_L[J] = I_L S\tau_L = 3.2\ \mathrm{kJ} \end{aligned} \tag{A19}$$

APPENDIX B: ELECTRON AND ION RELAXATION TIMES

The relaxation rates for electrons and for ions accordingly ν_{ee}, ν_{ii}, or equivalently the times τ_{ee}, τ_{ii}, that a species of particles reaches equilibrium, due to Coulomb collisions between electron–electron (ee) and separately ion–ion are given by (Eliezer, 2012):

$$\begin{aligned} \frac{1}{\nu_{ee}} &= \tau_{ee} = \left(\frac{3\sqrt{6}}{8\pi}\right)\frac{\sqrt{m_e}(k_B T_e)^{3/2}}{e^4 n_e \ln\Lambda_{ee}} \\ \frac{1}{\nu_{ii}} &= \tau_{ii} = \frac{1}{Z^4}\left\{\left(\frac{3\sqrt{6}}{8\pi}\right)\frac{\sqrt{m_i}(k_B T_i)^{3/2}}{e^4 n_i \ln\Lambda_{ii}}\right\} \end{aligned} \tag{A20}$$

Numerically, Eq. (A20) can be written

$$\begin{aligned} \tau_{ee}[s] &= 1.07\times 10^{10}\left(\frac{1}{n_e\ln\Lambda_{ee}}\right)[T_e(\mathrm{keV})]^{3/2} \\ \tau_{ii}[s] &= 4.58\times 10^{11}\left(\frac{1}{n_i\ln\Lambda_{ii}}\right)[T_i(\mathrm{keV})]^{3/2} \end{aligned} \tag{A21}$$

Regarding the fast ignition of a pre-compressed target with $n_e[\mathrm{cm}^{-3}] = 10^{26}$ and a laser pulse duration of 1 ps we have

https://doi.org/10.1017/S0263034615000701 Published online by Cambridge University Press

as order of magnitude estimates:

$$\begin{aligned}
&\tau_{ee}(\mathrm{DT}) \sim 10^{-17}[s](1\,\mathrm{keV}) - 10^{-15}[s](20\,\mathrm{keV})\\
&\tau_{ii}(\mathrm{DT}) \sim 4\times 10^{-16}[s](1\,\mathrm{keV}) - 4\times 10^{-14}[s](20\,\mathrm{keV})\\
&\tau_{ee}(p^{11}B) \sim 10^{-17}[s](1\,\mathrm{keV}) - 3\times 10^{-14}[s](50\,\mathrm{keV});\\
&\tau_{ii}(p^{11}B) \sim \frac{1}{Z^3}\left\{10^{-15}[s](1\,\mathrm{keV}) - 10^{-12}(200\,\mathrm{keV})[s]\right\}
\end{aligned} \tag{A22}$$

For the above numerical estimations we took $\ln\Lambda = 10$.

APPENDIX C: SHOCK WAVE INDUCED TWO TEMPERATURES MODEL

We use the non-relativistic shock wave equations to justify our two temperature model equations. In this case the kinetic energy W_k, the potential (internal) energy W_p and their appropriate power densities are related to the particle flow velocity u_p by:

$$\begin{aligned}
&\frac{W_k}{V}\left[\frac{\mathrm{erg}}{\mathrm{cm}^3}\right] = (\gamma-1)\rho c^2\left(\frac{t}{\tau_L}\right) = \frac{1}{2}\rho {u_p}^2\left(\frac{t}{\tau_L}\right)\\
&W_d = \frac{\mathrm{d}}{\mathrm{d}t}\left(\frac{W_k}{V}\right) = \frac{1}{2}\left(\frac{\rho {u_p}^2}{\tau_L}\right)
\end{aligned} \tag{A23}$$

$$\begin{aligned}
&U_p\left[\frac{\mathrm{erg}}{\mathrm{cm}^3}\right] = \frac{W_p}{V} = \frac{3}{2}nk_B T\\
&\frac{\mathrm{d}}{\mathrm{d}t}\left(\frac{W_p}{V}\right) = \frac{3}{2}k_B\frac{\mathrm{d}}{\mathrm{d}t}(nT) = \frac{3}{2}nk_B\frac{\mathrm{d}T}{\mathrm{d}t}
\end{aligned} \tag{A24}$$

At this stage we have one fluid with temperature and number density T and n, accordingly and neglect all losses or fusion energy creation. In the second equation in (A24) we have assumed that n does not change in time.

The 1D non-relativistic Hugoniot equations in the laboratory frame of reference, assuming a fluid initially at rest, are the following mass, momentum, and energy conservations

$$\begin{aligned}
&\rho_0 u_s = \rho(u_s - u_p)\\
&\rho_0 u_s u_p = P - P_0\\
&\rho_0 u_s\left(E - E_0 + \frac{1}{2}{u_p}^2\right) = P u_p
\end{aligned} \tag{A25}$$

The conservation energy of the third equation of (A25) can be written as

$$\begin{aligned}
&\mathrm{Pistonwork} = \mathrm{Internalenergy} + \mathrm{Kineticenergy}\\
&\mathrm{Pistonwork} = \int P\,dV = P(Su_p t)\\
&\mathrm{Internalenergy} = W_p = (\rho_0 S u_s t)(E - E_0)\\
&\mathrm{Kineticenergy} = W_K = (\rho_0 S u_s t)\left(\frac{1}{2}{u_p}^2\right)
\end{aligned} \tag{A26}$$

S is the cross-section area of the piston and E is the internal energy per unit mass. Since the initial pressure P_0 is negligible relative to the shock pressure P in our cases we get from the second and third equations of (A25)

$$\left.\begin{aligned}
&P u_p = \rho_0 u_s {u_p}^2\\
&P u_p = \rho_0 u_s\left(E - E_0 + \frac{1}{2}{u_p}^2\right)
\end{aligned}\right\} \Rightarrow \rho(E - E_0) = \frac{1}{2}\rho {u_p}^2 \tag{A27}$$

Inserting Eqs (A27) and (A26) into (A23) and (A24) we get for time independent density n,

$$\frac{3}{2}nk_B\frac{\mathrm{d}T}{\mathrm{d}t} = W_d \tag{A28}$$

During the time development of the temperature we have to take into account losses and the extra input energy due to nuclear fusion, namely

$$\frac{3}{2}nk_B\frac{\mathrm{d}T}{\mathrm{d}t} = W_d + f_\alpha W_f - \sum \mathrm{losses} \tag{A29}$$

Since we have two temperatures (at least) T_e and T_i we generalize Eq. (A29) to

$$\begin{aligned}
&\frac{3}{2}n_e k_B\frac{\mathrm{d}T_e}{\mathrm{d}t} = \eta_d W_d + f_\alpha \eta_f W_f - \sum_e \mathrm{losses}\\
&\frac{3}{2}n_i k_B\frac{\mathrm{d}T_i}{\mathrm{d}t} = (1-\eta_d) W_d + f_\alpha(1-\eta_f) W_f - \sum_i \mathrm{losses}
\end{aligned} \tag{A30}$$

This model is schematically described in Figure 4.

https://doi.org/10.1017/S0263034615000701 Published online by Cambridge University Press